

Introducing Protein Folding Using Simple Models

D. Thirumalai and D. K. Klimov

Department of Chemistry and Biochemistry and Institute for Physical Science and Technology

University of Maryland, College Park, MD 20742

Key Words: Biomolecular Folding, Symmetry, Designability, Evolution

I. INTRODUCTION

Most reactions in cells are carried out by enzymes [1]. In many instances the rates of enzyme-catalyzed reactions are enhanced by million fold. A significantly large fraction of all known enzymes are proteins which are made from twenty naturally occurring amino acids. The amino acids are linked by peptide bonds to form polypeptide chains. The primary sequence of a protein specifies the linear order in which the amino acids are linked. To carry out the catalytic activity the linear sequence has to fold to a well defined three dimensional structure. In cells only a relatively small fraction of proteins require assistance from chaperones (helper proteins) [2]. Even in the complicated cellular environment most proteins fold spontaneously upon synthesis. The determination of the three dimensional folded structure from the one dimensional primary sequence is the most popular protein folding problem.

For a number of years the protein folding problem remained only of academic interest. The synthesis of proteins in cells was described by Crick [1]. Schematically this process can be represented as $DNA \rightarrow RNA \rightarrow Proteins$. This proposal and Anfinsen's [3] demonstration that a denatured protein would fold to the native conformation under suitable conditions was sufficient to understand the role of protein folding in cells. However, in the last couple of decades many diseases have been directly linked to protein folding (especially misfolding) [4]. Thus, there is an urgency to understand the mechanisms in the formation of folded structures. Biotechnology industry is also interested in the problem because of the hope that by understanding the way polypeptide chains fold one can design molecules (using natural or synthetic constituents) of use in medicine. Finally, the full potential of the human genome project involves understanding what the genes encode. For all these profoundly important reasons the protein folding problem has taken center stage in molecular biology.

Because this problem is complex several venues of attack have been devised in the last fifteen years. A combination of experimental developments (protein engineering, advances in X-ray and NMR, various time resolved spectroscopies, single molecule manipulation methods) and theoretical approaches (use of statistical mechanics, computational strategies, use of simple models) [5–7] has lead to a greater understanding of how polypeptide chains reach the native conformation.

From our perspective there are four major problems that comprise the protein folding enterprise. They are:

a) Prediction of the three dimensional fold of a protein given only the amino acid sequence. This is referred to as the structure prediction problem. In Fig. (1) we show the three dimensional structure of myoglobin. The structure prediction problem involves determining this fold using the primary sequence which is given in the lower part of Fig. (1).

b) Given that a sequence folds to a known native structure what are the mechanisms in the transition from the unfolded conformation to the folded state? This is the kinetics problem whose solution requires elucidation of the pathways and transition states in the folding process.

c) How to design sequences that adopt a specified fold [8]? This is the inverse protein folding problem that is vital to the biotechnology industry.

d) There are some proteins that do not spontaneously reach the native conformation. In the cells these proteins fold with the assistance of helper molecules referred to as chaperonins. The chaperonin-mediated folding problem involves understanding the interactions between proteins.

It is not the aim of this chapter to introduce the reader to all the areas listed above. Our goal is modest. We describe some of the theoretical developments which arose from studies of caricatures of proteins. Such models were designed to understand certain general features about protein structures and how these are kinetically reached. To keep the bibliography compact we mostly cite review articles. The interested reader can find the original papers in these cited works. We hope that this short introduction will entice the reader to delve into the ever surprising world of biological macromolecules.

II. RANDOM HETEROPOLYMER AS A CARICATURE OF PROTEINS

In homopolymers all the constituents (monomers) are identical, and hence the interactions between the monomers and between the monomers and the solvent have the same functional form. To describe the shapes of a homopolymer (in the limit of large molecular weight) it is sufficient to model the chain as a sequence of connected beads. Such a model can be used to describe the shapes that a chain can adopt in various solvent conditions. A measure of shape is the dimension of the chain as a function of the degree of polymerization, N . If N is large then the precise chemical details do not affect the way the size scales with N [9]. In such a description a homopolymer is characterized in terms of a single parameter that essentially characterizes the effective interaction between the beads which is obtained by integrating over the solvent coordinates.

Proteins are clearly not homopolymers because many energy scales are required to characterize the polypeptide chain. Besides the excluded volume interactions and hydrogen bonds the potential between the side chain depend on the nature of the residues [1]. Therefore, as a caricature of proteins the heteropolymer model is a better approximation. A convenient limit is the random heteropolymer for which approximate analytic treatments are possible [10]. In a random heteropolymer the interactions between the beads are assumed to be randomly distributed. Some of the interactions are attractive (which is responsible for conferring globularity to the chain) while others are repulsive and these residues are better accommodated in an extended conformation. In proteins water is a good solvent for polar residues while it is poor solvent for hydrophobic residues. (In a good solvent contacts between the monomer and solvent are favored whereas in a poor solvent the monomers are

attracted to each other). Because only 55% of the residues in proteins are hydrophobic it is clear that in a typical protein energetic frustration plays a role. In addition because of chain connectivity there is also topological frustration. This arises because residues that are proximal tend to form structures on short length scales. Assembly of such short short length scale structures would typically be incompatible with the global fold giving rise to topological frustration. Even if energetic frustrations are eliminated a polypeptide chain (in fact biomolecules) are topologically frustrated [7].

In the field of spin glasses and structural glasses such frustration effects are well known [11]. Thus, it was natural to suggest that random heteropolymers could serve as a simple representation of polypeptide chains. In Appendix A we sketch computational details for one model of random heteropolymers. Bryngelson and Wolynes proposed, using phenomenological arguments, that the Random Energy Model (REM) would be an appropriate description of some aspects of proteins [12,5]. The rationale for this is the following: Consider the exponentially large number of conformations. Because of the presence of several conflicting energies in a polypeptide chain it is natural to assume that these energies are randomly distributed. If there are no correlations between these energies and if the distribution is Gaussian one gets the REM. Of course, in the REM model the chain connectivity is ignored and there is no manifest for a spatial dependence of the chain coordinates. We show in Appendix B that in the compact phase the random heteropolymer is equivalent to REM.

The random heteropolymer models of proteins are interesting from a statistical mechanical perspective. However, they do not explain the key characteristics of proteins such as reversible and cooperative folding to a unique native conformation. Moreover, the theories for heteropolymers suggest that typically the energy landscapes for these systems are extremely rugged consisting of many minima that are separated by barriers of varying heights [10]. This would mean that kinetically it would be impossible for chain with a typical realization of interactions to reach the ground state in finite time scales. Thus the dynamics of such random heteropolymer models typically exhibits glassy behavior. Natural proteins do not exhibit any hall mark of glassy dynamics at most temperatures of interest. It follows that a certain refinement of the random heteropolymers is required to capture protein-like properties. One of the important theoretical advances is the observation that very simple minimal models [13] can be constructed that capture many (not all) of the salient features observed in proteins [13]. The simplest manifestation of such models are the lattice representation of polypeptide chains. In the next section we introduce the models and describe a few results that have been obtained by numerically exploring their behavior.

III. LATTICE MODELS OF PROTEINS

The computational protocol for describing protein folding mechanisms is straightforward in principle. The dynamics are well described by the classical equations of motion. Simulations of a monomeric protein involves equilibrating the polypeptide chain in a box of water molecules at the desired temperature and density. If an appropriately long trajectory is generated then the dynamics of the protein can be directly monitored. There are two crucial limitations that prevent a straightforward application of this approach to study the folding of proteins. First, the interaction potentials or the force fields for such a complex system are not precisely known. Molecular dynamics simulations in the standard packages use po-

tentials that rely on the transferability hypothesis i.e., interactions designed in one context can be used in aqueous medium and for larger systems. The need to compute potentials that can be used reliably in the simulations of protein dynamics remains acute.

The second problem is related to the limitations in generating really long time trajectories that can sample all the relevant conformational space of proteins. To observe reversible folding of even a moderate sized protein requires simulations that span the millisecond time scale. More importantly making comparisons with experiments involves generating many (greater than perhaps 100) folding trajectories so that a reliable ensemble average is obtained. Thus, we need to make progress on both (force fields and enhanced sampling techniques in long time simulations) fronts before a straightforward all atom simulations become routine.

In light of the above mentioned difficulties various simplified models of proteins have been suggested [13]. The main rationale for using such drastic simplifications is that a detailed study of such models can enable us to decipher certain general principles that govern the folding of proteins [5–7]. For these class of models detailed computations without sacrificing accuracy is possible. Such an approach has yielded considerable insights into the mechanisms, time scales, and pathways in the folding of polypeptide chains. In this section we will outline some of the results that have been obtained (largely from our group) with the aid of simple lattice models of proteins.

In the simple version of the lattice representation of proteins the polypeptide chain is modeled as a sequence of connected beads. The beads are confined to the sites of a suitable lattice. Host of the studies have used cubic lattice. To satisfy the excluded volume condition only one bead is allowed to occupy a lattice site. If all the beads are identical we have a homopolymer model whose characteristics on lattices have been extensively studied. To introduce protein-like character the interactions between beads (ones separated by at least three bonds) that are near neighbors on a lattice are assumed to depend on the nature of the beads. The energy of a conformation, specified by $\{r_i, i = 1, 2, \dots, N\}$, is

$$E(\{r_i\}) = \sum_{i < j} \Delta(|r_i - r_j| - a) B_{ij} \quad (1)$$

where N is the number beads in the chain, a is the lattice spacing, and B_{ij} is the value of the contact interaction between beads i and j . We will consider different forms of B_{ij} . Since this model can be viewed as a coarse grained representation of the α -carbons of the polypeptide chain the value of a is typically taken to be about 3.8Å.

Lattice models have been used for a long time in polymer physics [14]. They were instrumental in computing many properties (scaling of the size of the polymer with N , distribution of end-to-end distance etc.) of real homopolymer chains. In the context of proteins lattice models were first introduced by Go and coworkers [15]. The currently popular Go model considers only interactions between residues (beads on the lattice) that occur in the native (ground) state. Thus, in this "strong specificity limit" only native contacts are taken into account. It follows that in this version of the Go model the chain is forced to adopt the lowest energy conformation at low temperatures. Go also considered a variant of this model in which certain non-native contacts are allowed. Although these models were insightful Go and coworkers did not use them to obtain plausible general principles of protein folding. This was partly due to the fact that in their studies they typically used long chains, and hence exact enumeration was not possible.

Simple lattice models, with the express purpose of obtaining minimal representations of polypeptide chains, were first suggested by Chan and Dill [16]. In order to account for the major interactions in proteins these authors argued that the twenty naturally occurring amino acids can be roughly divided into categories, namely, hydrophobic (H) and polar (P). Chan and Dill have suggested that this simple HP model can capture many salient features of proteins. They also suggested that many of the conceptual puzzles (Levinthal paradox in particular) could be addressed by systematically studying short chains. This simple exactly enumerable HP model and their variants have been used to understand cooperativity, folding kinetics, and designability of protein structures [13]. Thus, it is instructive to describe the calculations that have been done using lattice models. A study of such models indeed provides a good introduction to the computational aspects of protein folding.

Emergence of Structures: The sequence space of proteins is extremely dense. The number of possible protein sequences is 20^N . It is clear that even by the fastest combinatorial procedure only a very small fraction of such sequences could have been synthesized. Of course, not all of these sequences will encode protein structures which for functional purposes are constrained to have certain characteristics. A natural question that arises is how do viable protein structures emerge from the vast sea of sequence space? The two physical features of folded proteins are : (1) In general native proteins are compact but not maximally so. (2) The dense interior of proteins are largely made up of hydrophobic residues and the hydrophilic residues are better accommodated on the surface. These characteristics give the folded proteins a lower free energy in comparison to all other conformations.

Lattice models are particularly suited for answering the question posed above. We will show that the two physical restrictions are sufficient to rationalize the emergence of very limited (believed to be only on the order of a thousand or so) protein-like structures. To provide a plausible answer to this question using lattice models we need to specify the form of the interaction matrix elements B_{ij} . For purposes of illustration we consider the random bond (RB) model in which the elements B_{ij} are distributed as

$$P(B_{ij}) = \frac{1}{\sqrt{2\pi}\sigma} \exp\left[-\frac{(B_{ij} - B_0)^2}{2\sigma^2}\right]. \quad (2)$$

Here $\sigma(=1)$ is the variance in B_{ij} and the hydrophobicity parameter B_0 is the mean value. We chose $B_0 = 0$ (half the beads are hydrophobic) and $B_0 = -0.1$. The latter is motivated by the observation that in natural proteins roughly 55% of the residues are hydrophobic [17].

Protein-like structures are not only compact but also have low energy. With this in mind we have calculated the number of compact structures (CSs) as CSs with low energy for a given N . The number of CSs in its most general form may be written as

$$C_N(CS) \simeq \overline{Z}^N Z_1^{N\frac{d-1}{d}} N^{\gamma_c-1} \quad (3)$$

where $\ln \overline{Z}$ is the conformational free energy (in units of $k_B T$), Z_1 is the surface fugacity, d is the spatial dimension, and γ_c measures possible logarithmic corrections to the free energy. It is clear that natural proteins are relatively unique and hence their number on an average has to grow at rates that are much smaller than that given in Eq. (21). To explore this we have calculated by exact enumeration the number of compact structures, $C_N(CS)$ and the number of minimum energy compact structures $C_N(MES)$ as a function of N .

We performed exhaustive enumeration of all self-avoiding conformations, to explore the conformational space of the polypeptide chain of a given length. In order to reduce the sixfold symmetry on the cubic lattice we fixed the direction of the first monomeric bond in all conformations. The remaining conformations are related by eightfold symmetry on the cubic lattice (excluding the cases when conformations are completely confine to a plane or straight line). To decrease further the number of conformations to be analyzed the Martin algorithm [18] was modified to reject all conformations related by symmetry.

We define MES as those conformations, whose energies lie within the energy interval Δ above the lowest energy E_0 . Several values for Δ were used to ensure that no qualitative changes in the results are observed. We set Δ to be constant and equal to 1.2 (or 0.6) (definition (i)). We have also tested another definition for Δ , according to which $\Delta = 1.3|E_0 - tB_0|/N$, where t is the number of nearest neighbor contacts in the ground state (definition (ii)). It is worth noting that in the latter case Δ increases with N . Both definitions yield equivalent results. Using these definitions for Δ , we computed $C(\text{MES})$ as a function of the number of residues N .

The computational technique involves exhaustive enumeration of all self-avoiding conformations for $N \leq 15$ on cubic lattice. In doing so we calculated the energies of all conformations according to Eq. (19), and then determined the number of MES. Each quantity, such as the number of MES, $C(\text{MES})$, the lowest energy E_0 , the number of nearest-neighbor contacts t in the lowest energy structures, is averaged over 30 sequences. Therefore, when referring to these quantities, we will imply their average values. To test the reliability of the computational results an additional sample of 30 random sequences was generated. Note that in the case of $C(\text{MES})$ we computed the quenched averages, i.e., $C(\text{MES}) = \exp[\overline{\ln[c(\text{MES})]}]$, where c is the number of MES for one sequence.

The number of MES $C(\text{MES})$ is plotted as a function of the number of residues N in Fig. (2) for $B_0 = -0.1$ and $\Delta = 0.6$. A pair of squares at given N represents $C(\text{MES})$ computed for two independent runs of 30 sequences each. For comparison, the number of self-avoiding walks $C(\text{SAW})$ and the number of CS $C(\text{CS})$ are also plotted in this figure (diamonds and triangles, respectively). The most striking and important result of this graph is the following: As expected on general theoretical grounds, $C(\text{SAW})$ and $C(\text{CS})$ grow exponentially with N , whereas the number of MES $C(\text{MES})$ exhibits drastically different scaling behavior. There is no variation in $C(\text{MES})$ and its value remains practically constant within the entire interval of N starting with $N = 7$. We find (see Fig. (2)) that $C(\text{MES}) \approx 10^1$. This result further validates our earlier finding for two dimensional model. These results suggest that $C(\text{MES})$ grows (in all likelihood) only as $\ln N$ with N . Thus the restriction of compactness and low energy of the native states may force an upper bound on the number of distinct protein folds.

3D HP model: The calculations described above suggest that upon imposing minimal restrictions on the structures (compactness and low energies) the structure space becomes sparse. As suggested before this must imply that each basin of attraction (corresponding to a given MES) in the structure space must contain numerous sequences. The way these sequences are distributed among the very slowly growing number (with respect to N) of MES, i.e., the density of sequences in structure space, is an important question. This was beautifully addressed in the paper by Li *et. al* [19]. They considered a three dimensional ($N = 27$) cubic lattice. By using HP model and restricting themselves to only maximally compact

structures as putative native basins of attractions (NBA) they showed certain basins have much larger number of sequences. In particular, they discovered that one of the NBAs serves as a ground state for 3794 (total number is 2^{27}) sequences and hence was considered most designable (Fig. (3)). The precise density of sequences among the NBAs is clearly a function of the interaction scheme. These calculations and the arguments presented in the previous subsection using the random bond model point out that since the number of NBA for the entire sequence space is small it is likely that proteins could have evolved randomly. Naturally occurring folds must correspond to one of the basins of attraction in the structure space so that many sequences have these folds as the native conformations, i.e., these are highly designable structures in the language of LWC [19]. These ideas have been further substantiated by Lindgard and Bohr [20], who showed that among maximally compact structures there are only very few folds that have protein-like characteristics. These authors also estimated using geometrical characteristics and stability arguments that the number of distinct folds is on the order of a thousand. All of these studies confirm that the density of the structure space is sparse. Thus, each fold can be designed by many sequences. From the purely structural point of view nature does have several options in the sense that many sequences can be "candidate proteins". However, there is also evolutionary pressure to fold rapidly (i.e., a kinetic component to folding). This requirement further restricts the possible sequences that can be considered as proteins, because they must satisfy the dual criterion of reaching a definite fold on a biologically relevant time scale. These observations are schematically sketched in Fig. (4).

Symmetry and designability: In the study by Li. et. al. [19] it was noted that highly designable structures appear to be symmetric. Independently, in a thought provoking article Wolynes [21] has made a series of compelling arguments as to why nature might use symmetry (at least in an inexact manner) to generate symmetrical tertiary folds of proteins. Many enzymes are oligomers. Wolynes makes a number of observations about the symmetry aspects of protein structures: (a) The tetrameric hemoglobin (α -helical protein) molecule has an approximate two-fold symmetry. (b) A striking example of approximate symmetry in β proteins is found in the the structure of a monomeric γ crystallin in which the shapes adopted by residues 1-88 and 89-174 are nearly the same. However, the two individual sequences do not bear much similarity. This, of course, is consistent with the notion that the structure space is so sparse that many sequences are forced to adopt similar shapes. The interesting conclusion from examining the γ crystallin structure is that the underlying symmetries in the shape are only inexact. (c) The obvious example of very nearly symmetrical structures are in helical proteins with the the four helix bundle being one the most prominent examples (see Fig. (5)). (d) Various proteins with mixed topology (like TIM barrels and jelly rolls) appear to have the kind of inexact but apparent symmetrical arrangement discussed by Wolynes [22]. (e) He also conjectured that it is likely that the underlying approximate symmetry is reflected in the free energy landscape being funnel-like. This would facilitate rapid folding which for many proteins may be a result of evolutionary pressure. The precise connections between the symmetries and the folding mechanisms and functional competence of biological molecules have not been worked out. Nevertheless it appears that employing such ideas might be useful in *de novo* design of proteins.

We note that equally striking are the kind of symmetrical arrangements found in RNA molecules [23]. The crystal structure of the P4-P6 domain of *Tetrahymena* self-splicing RNA

clearly is highly symmetric with helices packed in a nearly regular arrangement. Since in an evolutionary sense the RNA world might have preceded the protein world it is interesting to speculate that the emergence of inexact design may have been a biological necessity. The observation of inexact symmetries in a protein structure might be a consequence of the fact that they are present in the "parent" molecules. In fact this evolutionary conservation may have been imprinted when evolution from RNA world to the current scheme for protein synthesis took place. The most compelling reason for observing near regular patterns in biomolecular structures is because synthesis of symmetrical folds might be energetically economical.

Exploring protein folding mechanism using lattice model: It is well known that proteins reach the biologically active native states in a relatively short time which is on the order of a second for most single domain proteins [1]. Based on folding and refolding experiments on ribonuclease A Anfinsen concluded that under appropriate conditions natural sequences of proteins spontaneously fold to their native conformation [3]. This implies that protein folding is self-assembly process i.e., the information needed for specifying the topology of the native state is contained in the primary sequence itself. This thermodynamic hypothesis does not, however, address the question of how the native state is accessed in a short time scale. This issue was raised by Levinthal who wondered how a polypeptide chain of reasonable length can navigate the astronomically large conformational space so rapidly. Levinthal posited that certain preferred pathways must guide the chain to the native state. The Levinthal paradox, simplistic as it is, has served as an intellectual impetus to understand the ease with which a polypeptide chain reaches the native conformation [5,6]. We use lattice models to describe the foldability of biological sequences of proteins. A sequence is foldable if it reaches the native state in a reasonable time and remains stable over some range of external conditions (pH, temperature).

Characteristic Temperatures: The basic features of folding can be understood in terms of two fundamental equilibrium temperatures that determine the "phases" of the system [7]. At sufficiently high temperatures (kT greater than all the attractive interactions) the shape of the polypeptide chain can be described as a random coil and hence its behavior is the same as a self-avoiding walk. As the temperature is lowered one expects a transition at $T = T_\theta$ to a compact phase. This transition is very much in the spirit of the collapse transition familiar in the theory of homopolymers [9]. The number of compact conformations at T_θ is still exponentially large. Because the polypeptide chains have additional energy scales that discriminate between the various compact conformations we expect a transition to the ground (native) state at a lower temperature T_F . Generally the transition at T_θ is second order, while the transition at T_F is first order like. Such transitions here are for very small systems and the notion of "phases" should be used with care. These expectations, based on fairly general arguments, have been confirmed in various lattice simulations of protein-like heteropolymers. For the lattice models the collapse temperature T_θ is determined from the peak of the specific heat and the folding transition temperature is obtained from the fluctuations in the overlap function given by

$$\Delta\chi = \langle \chi^2 \rangle - \langle \chi \rangle^2 \quad (4)$$

where

$$\chi = 1 - \frac{1}{N^2 - 3N + 2} \sum_{i < j+2} \delta(r_{ij}^{\vec{r}} - r_{ij}^N) \quad (5)$$

with r_{ij}^N referring to the native state. In Fig. (7a) (for the structure displayed in Fig. (6)) we plot the temperature dependence of C_v , which has a peak at $T_\theta = 0.83$. This figure also shows the variation of $d \langle R_g \rangle / dT$ with temperature. The peak of this curve (0.86) almost coincides with that of the specific heat indicating that this transition is associated with compaction of the chain. Hence, the maximum in C_v legitimately indicates the collapse temperature. X-ray scattering experiments have been used to obtain T_θ for a few proteins. In Fig. (7b) we show the temperature dependence of $\Delta\chi$ from which the folding temperature T_F is determined to be 0.79.

Folding Rates: The key question we want to answer is what are the intrinsic sequence dependent factors that not only determine the folding rates but also the stability of the native state? It turns out that many of the global aspects of folding kinetics of proteins can be understood in terms of the equilibrium transition temperatures. In particular, we will show that the key factor that governs the foldability of sequences is the single parameter

$$\sigma_T = \frac{T_\theta - T_F}{T_\theta} \quad (6)$$

which indicates how far T_F is from T_θ . To establish a direct correlation between the folding time τ_F and σ_T we generated a number of sequences for $N = 27$. The folding time was taken to be equal to the mean first passage time. The first passage for a given initial trajectory was calculated by determining the total number of Monte Carlo steps (MCS) needed to reach the native conformation for the first time. By averaging over an ensemble of initial trajectories (typically this number varies between 400-800 in our examples) the mean first passage time is obtained. The precise moves that are utilized in the simulations are described elsewhere [17]. The dependence of τ_F on σ_T (for the random bond model and for the other interaction schemes) is given in Fig. (8). This figure shows a remarkable correlation between the folding time and σ_T . A small change in σ_T results in a dramatic effect (a few orders of magnitude) on the folding times. It is clear that both T_θ and T_F are dependent on the sequence. As a result mutations that preserve the native state can alter the folding rates due to the change in the σ_T values.

Using lattice models we have also established that folding rates correlate well with $Z = (E_N - E_{MS})/\delta$, where E_N is the native state energy, E_{MS} is the average energy of the ensemble of misfolded structures, and δ is the dispersion in the contact energies. The relationship between σ and Z also suggests that, in general, the correlation between τ_F and σ should be superior. More importantly, experimental measurements of Z are difficult. On the other hand, both T_θ and T_F can be measured in scattering, CD, or fluorescence experiments. Other measures, such as energy gap (however, it is defined), do not correlate with τ_F .

In the previous section we showed that because the structure space is very sparse there have to be many sequences that map onto the countable number of basins in the structure

space. The kinetics here shows that not all the sequences, even for highly designable structures, are kinetically competent. Consequently, the biological requirements of stability and speed of folding severely restrict the number of evolved sequences for a given fold. This very important result is schematically shown in Fig. (4).

It is important to point out that the simulations reported in Fig. (8) were done at sequence dependent temperatures using the condition $\langle \chi(T_s) \rangle = 0.21$. At these temperatures, all of which are below their respective folding transition temperatures, the native conformation has the highest occupation probability. In lattice models the native state is a single conformation (a microstate) which is, of course, physically unrealistic. In real systems there is a volume associated with the native basin of attraction (NBA) and there are many conformations that map onto the NBA. The probability of being in the NBA at the various simulation temperatures is in excess of 0.5 so that under the conditions of our simulations the *stability criterion is automatically satisfied*. The results in Fig. (8), therefore, shows that the *dual requirement of stability and the kinetic accessibility* of NBA is most easily satisfied by those sequences that have small values of σ_T . Thus rapid folding occurs when $\sigma_T \approx 0$ i.e., near a multicritical-like point. In this case there are no detectable intermediate "phases". The sequence, whose native state is shown in Fig. (6) has $\sigma_T = 0.05$. We found that this sequence folds rapidly.

Topological Frustration and Kinetic Partitioning Mechanism: Lattice models can also be used to obtain the outlines of the mechanisms for folding of proteins. The qualitative aspects of the folding kinetics of biomolecules can be understood in terms of the concept of topological frustration. The primary sequence of proteins has about 55% hydrophobic residues. The linear density of hydrophobic residues along the polypeptide chain is roughly constant implying that the hydrophobic residues are spread throughout the chain. As a result on any length scale l there is a propensity for the hydrophobic residues to form tertiary contacts under folding conditions. The resulting structures which are formed by contacts between residues that are in proximity would be in conflict with the global fold corresponding to the native state. The incompatibility of structures on local scales with the near unique native state on the global scale leads to topological frustration. It is important to realize that topological frustration is inherent to all foldable sequences, and is a direct consequence of the polymeric nature of proteins as well as competing interactions (hydrophobic residues which prefer the formation of compact structures and hydrophilic residues which are better accommodated by extended conformations). A consequence of topological frustration is that the underlying energy landscape is rugged consisting of many minima that are separated by barriers of varying heights.

It is important to understand the nature of the low-lying minima in the rugged energy landscape. On the length scale l there are many ways of forming structures that are in conflict with the global fold. It is expected that most of these structures have high free energies and are unstable to thermal fluctuations. We expect a certain number of these structures to have low free energies and be relatively deep minima. The overlap between these structures and the native fold could be considerable and hence these structures could be viewed as being native-like. These competing basins of attraction (CBA) in which the polypeptide chain adopts native-like structures can act as kinetic traps that will slow down the folding process.

The basic consequences of topological frustration for mechanisms of folding can be understood in terms of the kinetic partitioning mechanism (KPM) [7]. Imagine an ensemble of denatured molecules in search of the native conformation. This is the experimental situation that arises when the concentration of denatured molecules is decreased. It is clear that a fraction of molecules Φ would reach the NBA rapidly without being trapped in the low lying energy minima. The remaining fraction would be trapped in the minima and only on longer time scales fluctuations enables the chain to reach the NBA. The value of the partition factor Φ depends on the sequence and is explicitly determined by the σ_T value. Thus because of topological frustration the initial pool of denatured molecules partitions into fast folders and slow folders that reach the native state by indirect off-pathway processes.

From the description of the kinetic partitioning mechanism (KPM) given above it follows that generically the time dependence of the fraction of molecules that have not folded at time t , $P_u(t)$, is given by

$$P_u(t) = \Phi \exp\left(-\frac{t}{\tau_{NCNC}}\right) + \sum_k a_k \exp\left(-\frac{t}{\tau_k}\right) \quad (7)$$

where τ_{NCNC} is the time constant for reaching the native state by the fast process, τ_k is the time for escape from the CBA labeled k , and a_k is the "volume" associated with the k^{th} CBA. From this consideration we expect that for a given sequence trajectories can be grouped into those that reach the native conformation rapidly (Φ being their fraction) and those that remain in one of the CBA for discernible length of time. In Fig. (9a) we show an example of trajectory that reaches the native state directly from the random coil conformation. In contrast in Fig. (9b) we show an example of a trajectory for the same sequence at the same simulation temperature. This figure shows that on a very short time scale the chain gets trapped in conformations other than the NBA and only on long time scale it reaches the native state. This figure illustrates the basic principle of KPM. If we perform an average over an ensemble of such trajectories the kinetic result given in Eq. (7) ensues.

Classifying Folding Mechanisms in terms of σ_T : The various folding mechanisms expected in foldable sequences may be classified in terms of the σ_T . We have already shown that sequences that fold extremely rapidly have very small values of σ_T . Based on our study of several model proteins as well as analysis of real proteins we classify the folding kinetics of proteins as follows [7]:

Fast Folders: For these sequences the value of σ_T is less than a certain small value σ_l . For such sequences the folding occurs directly from the ensemble of unfolded states to the NBA. The free energy surface is dominated by the NBA (or a funnel) and the volume associated with NBA is very large. The partition factor Φ is near unity so that these sequences reach the native state by two-state kinetics. The amplitudes a_k in Eq. (7) are nearly zero. There are no intermediates in the pathways from the denatured state to the native state. Fast folders reach the native state by a nucleation-collapse mechanism which means that once a certain number of contacts (folding nuclei) are formed then the native state is reached very rapidly [24,25]. The time scale for reaching the native state for fast folders (which are

normally associated with those sequences for which topological frustration is minimal) is found to be

$$\tau_{NCNC} = \frac{\eta a}{\gamma} f(\sigma_T) N^\omega \quad (8)$$

where η is the solvent viscosity, a is the typical size of a residue, γ is the average surface tension between the residue and water, $f(\sigma_T)$ is typically an exponential function of σ_T , and the exponent ω is between 3.8 and 4.2. In general, only small proteins (N less than about 100) are fast folders.

Moderate Folders: Sequences for which $\sigma_l \leq \sigma_T \leq \sigma_h$ can be classified as moderate folders. Unlike fast folding sequences the Φ values are fractional which means that a substantial fraction of molecules is essentially trapped in one of the CBAs for some length of time. For these sequences there are detectable intermediates and for all but very small proteins the rate determining step is the activated transition from one of the CBAs to the native state. The average time scale for transition from these misfolded structures to the native conformation is given by

$$\tau_F \approx \tau_0 \exp(\sqrt{N}) \quad (9)$$

at $T \approx T_F$. This shows that typical barriers for moderate folders are quite small. As a result the folding times even for long proteins ($N \approx 200$) are only on the order of a second. It is these small barriers that enable typical proteins to fold in biologically relevant time scale without encountering the Levinthal paradox.

Slow Folders and Chaperones: For sequences with $\sigma_T \geq \sigma_h$ folding is extremely slow and these sequences may not reach the native state in a biologically relevant time scales. The volume corresponding to NBA is very small in this case and as a result Φ is nearly zero. The free energy surface is dominated by CBAs. Under these circumstances spontaneous folding does not become viable. In cells such proteins are rescued by chaperones. Typically this happens when N is so large that $\tau_0 \exp(\sqrt{N})$ exceeds reasonable folding time scales. Thus in cells we expect that only those proteins which are large or whose biological functioning state has to be oligomers require chaperones.

Minimum number of residues for obtaining foldable protein structures: Natural proteins are made up of twenty amino acid residues. An important question, from the perspective of protein design, is how many distinct types of residues are required for protein-like behavior? Such a selection cannot be made arbitrarily because in natural proteins one should have polar, hydrophobic, and charged residues. In addition, for optimal packing of the core hydrophobic residues with different van der Waals radii may be required. To explore the potential simplification of the number of residues Wang and Wang [26] have carried out a highly significant study using lattice models and standard statistical potentials for the contact interaction elements B_{ij} (Eq. (19)). They discovered that a grouping of amino acid residues into five categories mimics the folding behavior found using the standard twenty residues. To demonstrate this they used a cubic lattice with $N = 27$, and mostly focussed on the maximally compact structures as ground states. Thus, structures such as ones given

in Fig. (6) are not explicitly considered. Nevertheless, the demonstration that a suitable set of five amino acid residue types is sufficient is an important result which should have implication for protein design problem - the generation of primary sequences that can fold to a chosen target folded structure.

In their original article they mostly focussed on various thermodynamic properties (nature and degeneracy of the ground states). They have also carried out kinetic simulations to assess if the kinetic properties are altered by using a reduced number of residues. To test this idea Wang and Wang used the foldability index σ (which correlates well with fold rates) as a discriminator of sequence properties. The precise question addressed by Wang and Wang is the following: What is the minimum number of residues that are required to obtain foldable (characterized by having relatively small values of σ) sequences? We find that fast folding sequences have σ less than about a quarter. They carried out two sets of computations. In one set they initially optimized the stability gap [5] of various sequences using the twenty residues. They substituted the residues in these optimized sequences by the representative residue for each group. Four subgroups were considered with each containing five and a variant, three and two amino acids. The foldability index for the standard sample and their substitutes is shown in Fig. (10) as solid circle. In another set of computations they examined the foldability index (open diamonds in Fig. (10)) for sequences that were optimized using the reduced sets of amino acids. Both these curves show that as long as the number of amino acid types exceed five one can generate sequences with relatively small values of σ . Fig. (10) also shows that smaller values of σ can be obtained if optimization is carried out with reduced sets of amino acids. Such sequences are foldable i.e, the dual requirements of stability over a wide temperature range and the kinetic accessibility of their native states are simultaneously satisfied.

IV. CONCLUSIONS

The examples of modeling discussed in Sections (II) and (III) are meant to illustrate the ideas behind theoretical and computational approaches to protein folding. It should be borne in mind that we have discussed only a very limited aspect of the rich field of protein folding. The computations described in Section (III) can be carried out easily on a desktop computer. Such an exercise is, perhaps, the best of way of appreciating the simple approach to get at the principles that govern the folding of proteins.

In this chapter we have not discussed experimental advances that are offering extraordinary insights into the way the denatured molecules reach the native state. Two remarkable experimental approaches hold the promise that in short order we will be able to watch the folding process from submicrosecond time scale till the native state is reached. A brief summary of these follow.

1) Eaton and coworkers showed in 1993 that optical triggers of folding can offer a window into the folding process from microsecond time scale [27]. Since this pioneering work many laboratories have probed the plausible structure formation that occur on short time scale. Fast folding experimental techniques have been used to obtain detailed kinetics for the building blocks of proteins, namely, β -hairpin, α -helices, and loops. Very recent experiments have given compelling evidence that there are populated native-like intermediates even in proteins that were thought to follow two-state kinetics.

2) Perhaps the most exciting development in the last few years is the ability to nanomanipulate single biomolecules using atomic force microscopy and optical tweezer techniques [28]. So far such experiments have been used to provide a microscopic basis of elasticity in muscle proteins. If these stretching experiments can be combined with fluorescent resonance energy transfer experiments then it is possible to follow the folding of individual molecules as it passes through the transition state to the native conformation. It has been suggested on theoretical grounds that such two-dimensional single molecule experiments can measure directly the distribution of folding rates (and the barrier distribution) in much the same way mean first passage times are computed in minimal protein models (see Section (III)).

The challenges posed by these high precision experiments demand more refined models and further developments in computational techniques. For the theoretically inclined it will no longer be sufficient to describe kinetics only in terms of energy landscapes. The wealth of data that are being generated by experiments, such as the ones mentioned above, requires quantitative understanding of the various factors that govern the pathways, mechanisms, and the transition states in the folding process. These challenging issues will make the area of biomolecular folding an engaging one for many years to come.

ACKNOWLEDGMENTS

We are grateful to John D. Weeks for useful comments and to Chao Tang for supplying Fig. (3). We are indebted to Dr. J. Wang and Prof. W. Wang for kindly providing us with Figure (10) prior to publication.

APPENDIX A:

There are several versions of the random heteropolymer models. To keep the discussions technically simple we will consider one case - the so called random hydrophilic-hydrophobic chain whose phases were studied by Garel, Orland and Leibler (GLO) [10]. The GLO model consists of a polymer chain with N monomers. The GLO model can be viewed as a generalization of the popular Edwards model which was introduced to understand swelling of real homopolymer chains in good solvents [9]. In the GLO model the chain is made up of hydrophobic (hydrophilic) residues that tend to collapse (swell) the chain when dispersed in a solvent. The solvent mediated interactions at each site is assumed to be random. The random interactions depend only on a given site i and the strength depends on the degree of hydrophilicity λ_i . Besides the term accounting for chain connectivity there are two and higher body interactions that determine the shape of the chain. In the GLO model the two body interaction is given by

$$v_{ij} = v_0 + \beta(\lambda_i + \lambda_j)\delta[r_i - r_j] \quad (\text{A1})$$

where v_0 is repulsive short range interaction, λ_i is a quenched random variable which is distributed as

$$P(\lambda_i) = \frac{1}{\sqrt{2\pi\sigma^2}} \exp\left[-\frac{(\lambda_i - \lambda_0)^2}{2\sigma^2}\right]. \quad (\text{A2})$$

If the mean λ_0 is positive then the majority of the residues are hydrophilic. Description of the collapsed phase of the chain requires introducing three and four-body interaction terms. Thus, the total Hamiltonian is

$$\beta H = \frac{1}{2} \sum_{i \neq j} v_{ij} + \frac{1}{6} \sum_{i \neq j \neq k} \omega_3 \delta(r_i - r_j) \delta(r_i - r_k) + \frac{1}{24} \sum_{i \neq j \neq k \neq l} \omega_4 \delta(r_i - r_j) \delta(r_j - r_k) \delta(r_k - r_l). \quad (\text{A3})$$

Since the charge variables λ_i are quenched the thermodynamics of the system requires averaging the free energy using the distribution $P(\lambda_i)$ i.e.,

$$F = -k_B T \int \prod P(\lambda_i) \ln Z(\lambda_i) d\{\lambda_i\}. \quad (\text{A4})$$

The average of $\ln Z(\lambda_i)$ is most conveniently done using the replicas through the relation

$$\ln Z = \lim_{n \rightarrow 0} \frac{Z^n - 1}{n}. \quad (\text{A5})$$

Using Eqs. (2-4) the required average can be carried out. This leads to a complicated expression for $\overline{Z^n}$ where the bar indicates the average over the quenched random variables λ_i . In terms of the order parameters

$$q_{ab}(r, r') = \int ds \delta(r_a(s) - r) \delta(r_b(s) - r') \quad (\text{A6})$$

and

$$\rho_a(r) = \int ds \delta(r_a(s) - r) \quad (\text{A7})$$

(a and b are replica indices) the expression for $\overline{Z^n}$ becomes

$$\overline{Z^n} = \int Dq_{ab}(r, r') D\hat{q}_{ab}(r, r') D\rho_a(r) D\phi_a(r) \exp[H_{eff}] \quad (\text{A8})$$

where

$$H_{eff} = G(q_{ab}, \hat{q}_{ab}, \rho_a, \phi_a) + \ln \zeta(\hat{q}_{ab}, \phi_a) \quad (\text{A9})$$

with

$$G = \int dr \sum (i\rho_a \phi_a - (v_0 + 2\beta\lambda_0) \frac{\rho_a^2}{2} - \frac{\omega_3'}{6} \rho_a^3 - \frac{\omega_4}{24} \rho_a^4) \\ + \int dr \int dr' \sum_{a < b} (iq_{ab}(r, r') \hat{q}_{ab}(r, r') + \beta^2 \lambda^2 q_{ab}(r, r') \rho_a(r) \rho_b(r'))$$

and

$$\zeta(\hat{q}_{ab}, \phi_a) = \int \prod_a Dr_a(s) \exp(-H_T\{r_a(s)\}). \quad (\text{A10})$$

In Eq. (10) $H_T\{r_a(s)\}$ is

$$H_T\{r_a(s)\} = \exp\left[-\frac{d}{2a^2} \int_0^N ds \sum_a \left(\frac{dr}{ds}\right)^2 - i \int_0^N ds \sum_a \phi_a(r_a(s)) - i \int_0^N ds \sum_{a < b} \hat{q}_{ab}(r_a, r_b)\right]. \quad (\text{A11})$$

and

$$\omega_3' = \omega_3 - 3\beta^2\lambda^2. \quad (\text{A12})$$

The path integrals in Eq. (10) may be evaluated using the spectrum of the effective n-body Hamiltonian

$$H_n = -\frac{d}{2a^2} \sum_a \nabla_a^2 + \sum_a i\phi(r_a) + \sum_{a < b} i\hat{q}_{ab}(r_a, r_b) \quad (\text{A13})$$

in the limit of $n \rightarrow 0$. If N is very large then we can use ground state dominance to evaluate the spectrum of H_n . This gives

$$\varsigma(\hat{q}_{ab}, \phi_a) \simeq \exp[-N \min_{\{\Psi(r)\}} \{ \langle \Psi | H_n | \Psi \rangle - E_0(\langle \Psi | \Psi \rangle - 1) \}] \quad (\text{A14})$$

where E_0 is the ground state energy of H_n . GLO evaluated the integral over q_{ab} (Eq. (6)) by a saddle point approximation which leads to

$$i\hat{q}_{ab}(r, r') = -\beta^2\lambda^2\rho_a(r)\rho_b(r'). \quad (\text{A15})$$

From the above equation it follows that in the mean-field limit replica symmetry is not broken. This makes the GLO model conceptually simpler to interpret than the random bond heteropolymer model discussed in the Appendix.

The total wavefunction $\Psi\{r_1, r_2, \dots, r_n\}$ (Eq. (12)) is written as a product of single particle functions (Hartree approximation). The various integrals are evaluated in the saddle point approximation. A simple Gaussian form for the trial one particle wavefunction

$$\phi(r) = \left(\frac{1}{2\pi R^2}\right)^{\frac{d}{4}} \exp\left(-\frac{r^2}{2R^2}\right) \quad (\text{A16})$$

is chosen with R being the single variational parameter. Upon performing the Gaussian integrals the free energy per monomer f becomes

$$\beta f = \frac{a^2}{8R^2} + \frac{1}{(2\sqrt{\pi})^d} \frac{(v_0 + 2\beta\lambda_0)}{2} \frac{N}{R^d} + \Omega \quad (\text{A17})$$

where

$$\Omega = \left(\frac{1}{(2\pi\sqrt{3})^d} \frac{\omega_3}{6} - \left(\frac{1}{2\pi}\right)^d (3^{-d/2} - 2^{-d})\right) \left(\frac{N}{R^d}\right)^2 + \left(\frac{1}{(32\pi^3)}\right)^{d/2} \frac{\omega_4}{24} \left(\frac{N}{R^d}\right)^3. \quad (\text{A18})$$

At low temperatures the shape of the chain is determined by the sign of first term in Eq. (18). If the sign is negative then the positive four body term is required for a stable theory.

The phase of the random hydrophobic-hydrophilic model is complicated and depends on the value of λ_0 [10]. We only describe the hydrophilic case when λ_0 is positive. In this case

there is a first order transition to a collapsed state ($R \sim N^{-1/d}$) induced by the negative three body term. GLO pointed out that this transition is neither the usual θ -point nor is it a freezing temperature because there is no replica symmetry breaking. In fact, this collapse transition resembles that seen in proteins where it is suspected that it is first order transition. The microscopic origin of the first order transition upon collapse of polypeptide chains is not fully understood. Recent arguments, suggest that it could arise because burial of hydrophobic residues and accommodation of the hydrophilic ones at the surface of proteins in water requires some work and perhaps this assembly happens in a discontinuous manner.

APPENDIX B:

In Section (II) we considered a variational-type theory to treat the thermodynamics of the random hydrophobic-hydrophilic heteropolymer. Here we describe a limiting behavior of the random bond model [29]. In this appendix we show that the random bond model in the compact phase is identical to the Random Energy Model (REM). Historically, REM was proposed as caricature for proteins on phenomenological grounds [12]. The heteropolymer with random bond interactions was treated using a variational theory which suggested that when the disorder increases beyond a limiting value the chain undergoes a thermodynamic glass transition. The nature of this transition is closely related to Potts glasses.

The random-bond heteropolymer is described by a Hamiltonian similar to Eq. (1) except the short range two-body term v_{ij} is taken to be random with a Gaussian distribution. In this case a three-body term with a positive value of ω_3 is needed to describe the collapsed phase. The Hamiltonian is

$$H = \sum_{i < j} (v_0 + v_{ij}) \delta(r_i - r_j) + \sum_{i \neq j \neq k} \delta(r_i - r_j) \delta(r_j - r_k) \quad (\text{B1})$$

The distribution of the random couplings is given by

$$P(v_{ij}) = \frac{1}{\sqrt{2\pi v^2}} \exp\left(-\frac{v_{ij}^2}{2v^2}\right). \quad (\text{B2})$$

In the collapse phase the monomer density $\rho = \frac{N}{R^3}$ is constant (for large N). Thus, the only conformation dependent term in Eq. (A1) comes from the random two-body term. Because this term is linear combination of Gaussian variables we expect that its distribution is also Gaussian and hence, can be specified by the two moments. Let us calculate the correlation $\overline{E_1 E_2}$ between the energies E_1 and E_2 of two conformations $\{r_i^{(1)}\}$ and $\{r_i^{(2)}\}$ of the chain in the collapsed state. The mean square of E_1 is

$$\overline{E_1^2} = \frac{v^2}{2} \sum_{i,j} \delta(r_i^{(1)} - r_j^{(1)}) = \frac{v^2}{2} N \rho \quad (\text{B3})$$

which is independent of the collapsed conformation. Similarly, we have

$$\begin{aligned} \overline{E_1 E_2} &= \frac{v^2}{2} \sum_{i,j} \delta(r_i^{(1)} - r_j^{(1)}) \delta(r_i^{(2)} - r_j^{(2)}) \\ &= \frac{v^2}{2} \sum_{r,r'} q_{12}^2(r, r') \end{aligned}$$

where $q_{12}(r, r')$ is the overlap between the two conformations. Because

$$\sum_{r, r'} q_{12}(r, r') = N \quad (\text{B4})$$

and since the monomer density is constant we $q_{12}(r, r') = \frac{\rho^2}{N}$. This implies

$$\overline{E_1 E_2} = \frac{v^2}{2} \rho^2. \quad (\text{B5})$$

Thus the joint probability is

$$\lim_{N \rightarrow \infty} \sim \exp\left(-\frac{E_1^2 + E_2^2}{N \rho v^2}\right) \quad (\text{B6})$$

which is equivalent the behavior in uncorrelated REM. Thus, it is not a surprise that in large dimensions (which are captured by variational type treatments) the random bond heteropolymer model yields exactly the same result as the REM.

REFERENCES

- [1] L. Stryer. *Biochemistry*. W. H. Freeman, 1988.
- [2] G. H. Lorimer. A quantitative assessment of the role of the chaperonin proteins in protein folding *in vivo*. *FASEB J*, 10:5–9, 1996.
- [3] C. B. Anfinsen. Principles that govern the folding of protein chains. *Science*, 181:223–230, 1973.
- [4] P. T. Lansbury. Evolution of amyloids: What normal protein folding can tell us about fibrillogenesis and disease. *Proc. Natl. Acad. Sci. (USA)*, 96:3342–3344, 1999.
- [5] J. N. Onuchic, Z. A. Luthey-Schulten, and P. G. Wolynes. Theory of protein folding: An energy landscape perspective. *Ann. Rev. Phys. Chem.*, 48:545–600, 1997.
- [6] K. A. Dill and H. S. Chan. From Levinthal to pathways to funnels. *Natur. Struct. Biol.*, 4:10–19, 1997.
- [7] D. Thirumalai and D. K. Klimov. Deciphering the timescales and mechanisms of protein folding using minimal off-lattice models. *Curr. Opin. struct. Biol.*, 9:197–207, 1999.
- [8] E. Shakhnovich. Protein design: a perspective from simple tractable models. *Folding & Design*, 3:R45–R58, 1998.
- [9] P. G. deGennes. *Scaling Concepts in Polymer Physics*. Cornell University Press, 1985.
- [10] T. Garel, H. Orland, and D. Thirumalai. Analytical theories of protein folding. In R. Elber, editor, *New Developments in Theoretical Studies of protein folding*, pages 197–268. Singapore, World Scientific, 1996.
- [11] M. Virasoro M. Mezard and G. Parisi. *Spin glass theory and beyond*. World Scientific, 1987.
- [12] J. D. Bryngelson and P. G. Wolynes. Spin glasses and the statistical mechanics of protein folding. *Proc. Natl. Acad. Sci. (USA)*, 84:7524–7528, 1987.
- [13] K. A. Dill, S. Bromberg, K. Yue, K. M. Fiebig, D. P. Yee, P. D. Thomas, and H. S. Chan. Principles of protein folding - a perspective from simple exact models. *Protein Science*, 1995:561–602, 1995.
- [14] W. J. C. Orr. Statistical treatment of polymer solutions at infinite dilution. *Tran. Faraday Soc.*, 43:12–27, 1947.
- [15] H. Taketomi, Y. Ueda, and N. Go. Studies on protein folding, unfolding, and fluctuations by computer simulation. *Int. J. Pept. Protein Res.*, 7:445–459, 1975.
- [16] H. S. Chan and K. A. Dill. Intrachain loops in polymers: effects of excluded volume. *J. Chem. Phys.*, 90:493–509, 1989.
- [17] D. K. Klimov and D. Thirumalai. Factors governing the foldability of proteins. *Proteins: Struct. Funct. Genet.*, 26:411–441, 1996.
- [18] D. Thirumalai and D. K. Klimov. Emergence of stable and fast folding protein structure. In S. Kim, K. J. Lee, and W. Sung, editors, *Stochastic dynamics and Pattern Formation in Biological and Complex Systems*, pages 95–111. Melville, New York, American Institute of Physics, 2000.
- [19] H. Li, N. Winfree, and C. Tang. Emergence of preferred structures in a simple model of protein folding. *Science*, 273:666–669, 1996.
- [20] Per-Anker Lindgard and H. Bohr. Magic numbers in protein structures. *Phys. Rev. Letters*, 77:779–782, 1996.
- [21] P. G. Wolynes. Symmetry and the energy landscape of biomolecules. *Proc. Natl. Acad. Sci. (USA)*, 93:14249–14255, 1996.

- [22] P. G. Wolynes. Folding nucleus and energy landscapes of larger proteins within the capillarity approximation. *Proc. Natl. Acad. Sci. USA*, 94:6170–6175, 1997.
- [23] J.H. Cate, A.R. Gooding, E. Podell, K. Zhou, B.L. Golden, C.E. Kundrot, T.R. Cech, and J.A. Doudna. Crystal structure of a group i ribozyme domain: Principles of rna packing. *Science*, 273:1678–1685, 1996.
- [24] Z. Guo and D. Thirumalai. Kinetics of protein folding: Nucleation mechanism, time scales and pathways. *Biopolymers*, 36:83–103, 1995.
- [25] E. I. Shakhnovich, V. Abkevich, and E. I. Shakhnovich. Conserved residues and the mechanism of protein folding. *Nature*, 379:96–98, 1996.
- [26] J. Wang and W. Wang. A computational approach to simplifying the protein folding alphabet. *Nat. Struct. Bio.*, 6:1033–1038, 1999.
- [27] W.A. Eaton, V. Munoz, P.A. Thompson, E.R. Henry, and J. Hofrichter. Kinetics and dynamics of loops, α -helices, β -hairpins, and fast-folding proteins. *Acc. Chem. Res.*, 31:745–753, 1998.
- [28] T.E. Fisher, A.F. Oberhauser, M. Carrion-Vazquez, P.E. Marszalek, and J.M. Fernandez. The study of protein mechanics with the atomic force microscope. *Trends in Biochemical Sciences*, 24:379–384, 1999.
- [29] E. Shakhnovich and A. Gutin. Formation of unique structure in polypeptide chains. theoretical investigation with the aid of replica approach. *Biophysical Chemistry*, 34:187–199, 1989.
- [30] R. Sayle and E.J. Milner-White. Rasmol: Biomolecular graphics for all. *Trends in Biochemical Sciences*, 20:374–376, 1995.

FIGURES

Fig. (1) The 3D native structure of hemoglobin visualized using RasMol 2.6 [30]. The linear sequence of amino acids of hemoglobin is given below the figure.

Fig. (2) Scaling of the number of MES $C(\text{MES})$ (squares) is shown for the hydrophobic parameter $B_0 = -0.1$ and $\Delta = 0.6$. Data are obtained for the cubic lattice. The pairs of squares for each N represent the quenched averages for different samples of 30 sequences. The number of compact structures $C(\text{CS})$ and self-avoiding conformations $C(\text{SAW})$ are also displayed to underscore the dramatic difference of scaling behavior of $C(\text{MES})$ and $C(\text{CS})$ (or $C(\text{SAW})$). It is clear that $C(\text{MES})$ remains practically flat, i.e. it grows no faster than $\ln N$.

Fig. (3) Histogram of number of structures with a given number of associated sequences N_s for 3D 3x3x3 case, in a log-log plot.

Fig. (4) Schematic illustration of the stages in the drastic reduction of sequence space in the process of evolution to functionally competent protein structures.

Fig. (5) Native structure of acyl-coenzyme A binding protein (first NMR structure out of 29 deposited to PDB). The figure was created using RasMol 2.6 [30].

Fig. (6) The native conformation of fast folding sequence ($N = 27$) with random bond potentials is shown. This structure has $c = 22$ non-bonded contacts, therefore it is not a maximally compact conformation for which $c = 28$. The figure was created using RasMol 2.6 [30].

Fig. (7) (a) Thermodynamic functions computed for the sequence whose native state is shown in Fig. (3). (a) Specific heat C_v (dotted line) and derivative of the radius of gyration with respect to temperature dR_g/dT (dashed line) as a function of temperature. The collapse temperature T_θ is determined from the peak of C_v and found to be 0.83. T_θ is very close to the temperature, at which dR_g/dT becomes maximum (0.86). This illustrates that T_θ is indeed associated with the compaction of the chain. Temperature dependence of fluctuations of overlap function $\Delta\chi$ is given by solid line. The folding transition temperature T_F is obtained from the peak of $\Delta\chi$ and for this sequence $T_F = 0.79$. The curves are scaled to fit one plot.

(b) Time dependence of the fraction of unfolded molecules $P_u(t)$ for the sequence 74 calculated at folding conditions $T_s \lesssim T_F$. The function $P_u(t)$ is computed from a distribution of first passage times τ_{1i} . First passage time for a given initial condition is the first time the trajectory reaches the native conformation. Typically an adequately converged distribution is obtained by averaging over several hundred initial conditions. For the conditions used in this simulation folding is two-state, therefore, $P_u(t)$ is adequately fit with the single exponential (thick solid line). The folding time τ_F obtained from the fit is $1.4 \times 10^6 \text{ MCS}$.

Fig. (8) Plot of the folding times τ_F as a function of σ_T for the 22 sequences. This figures shows that under the external conditions when the NBA is the most populated there is a remarkable correlation between τ_F and σ_T . The correlation coefficient is 0.94. It is clear that over a four orders of magnitude of folding times $\tau_F \approx \exp(-\sigma_T/\sigma_0)$ where σ_0 is a constant. In both panels the filled and open circles are for the RB and KGS 27-mer models, respectively. The open squares are for $N = 36$.

Fig. (9) Examples of folding trajectories at $T = T_s$ derived from the condition $\langle \chi(T_s) \rangle = 0.21$. (a) Fast folding trajectory as monitored by $\chi(t)$. It is seen that sequence reaches the

native state very rapidly in a two-state manner without being trapped in intermediates. The first passage time for this trajectory is 277,912 MCS. (b) Slow folding trajectory for the same sequence. The sequence becomes trapped in several intermediate states with large χ en route to the native state. The first passage time is 11,442,793 MCS. Notice that the time scales in both panels are dramatically different.

Fig. (10) The figure gives the foldability σ of 27-mer lattice chains with sets containing different number of amino acids. The sets are generated according to scheme described in [26]. The set of 20 amino acids is taken as a standard sample. Each sequence with 20 amino acids is optimized to fulfill the stability gap [5]. The residues in the standard samples are substituted with four different sets containing smaller number of amino acids [26]. The foldability of these substitution are indicated by the solid circles. The open diamonds correspond to the sequences with same composition. However, the amino acids are chosen from the reduced representation and the result sequence is optimized using the stability gap [5].



1val - 2leu - 3ser - 4pro - 5ala - 6asp - 7lys - 8thr - 9asn - 10val - 11lys
 12ala - 13ala - 14trp - 15gly - 16lys - 17val - 18gly - 19ala - 20his - 21ala - 22gly
 23glu - 24tyr - 25gly - 26ala - 27glu - 28ala - 29leu - 30glu - 31arg - 32met - 33phe
 34leu - 35ser - 36phe - 37pro - 38thr - 39thr - 40lys - 41thr - 42tyr - 43phe - 44pro
 45his - 46phe - 47asp - 48leu - 49ser - 50his - 51gly - 52ser - 53ala - 54gln - 55val
 56lys - 57gly - 58his - 59gly - 60lys - 61lys - 62val - 63ala - 64asp - 65ala - 66leu
 67thr - 68asn - 69ala - 70val - 71ala - 72his - 73val - 74asp - 75asp - 76met - 77pro
 78asn - 79ala - 80leu - 81ser - 82ala - 83leu - 84ser - 85asp - 86leu - 87his - 88ala
 89his - 90lys - 91leu - 92arg - 93val - 94asp - 95pro - 96val - 97asn - 98phe - 99lys
 100leu - 101leu - 102ser - 103his - 104cys - 105leu - 106leu - 107val - 108thr - 109leu - 110ala
 111ala - 112his - 113leu - 114pro - 115ala - 116glu - 117phe - 118thr - 119pro - 120ala - 121val
 122his - 123ala - 124ser - 125leu - 126asp - 127lys - 128phe - 129leu - 130ala - 131ser - 132val
 133ser - 134thr - 135val - 136leu - 137thr - 138ser - 139lys - 140tyr - 141arg

Fig. (1)

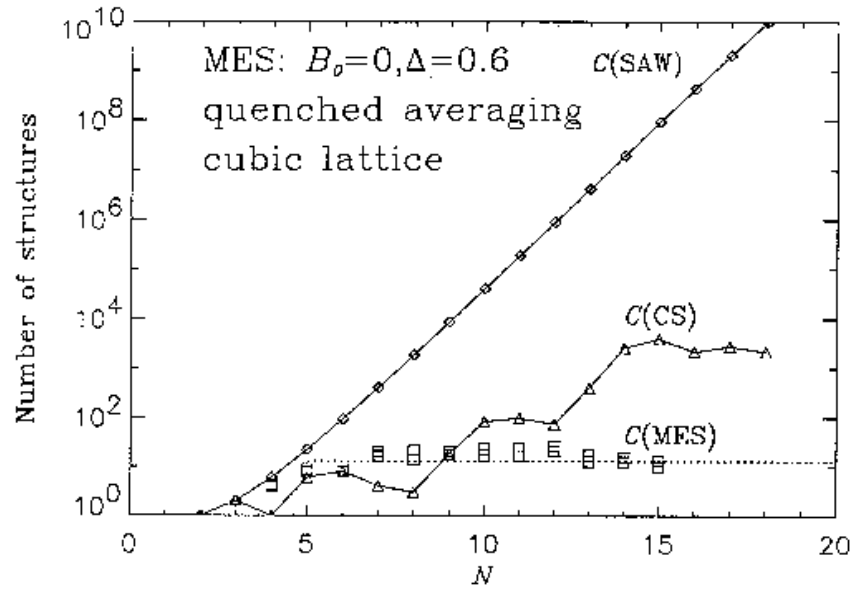


Fig. (2)

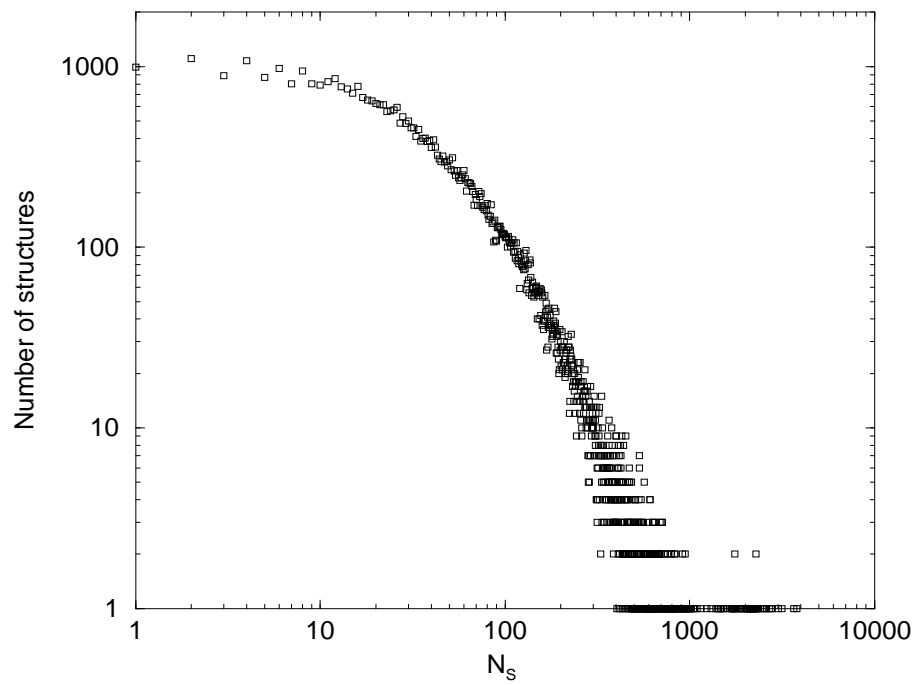


Fig. (3)

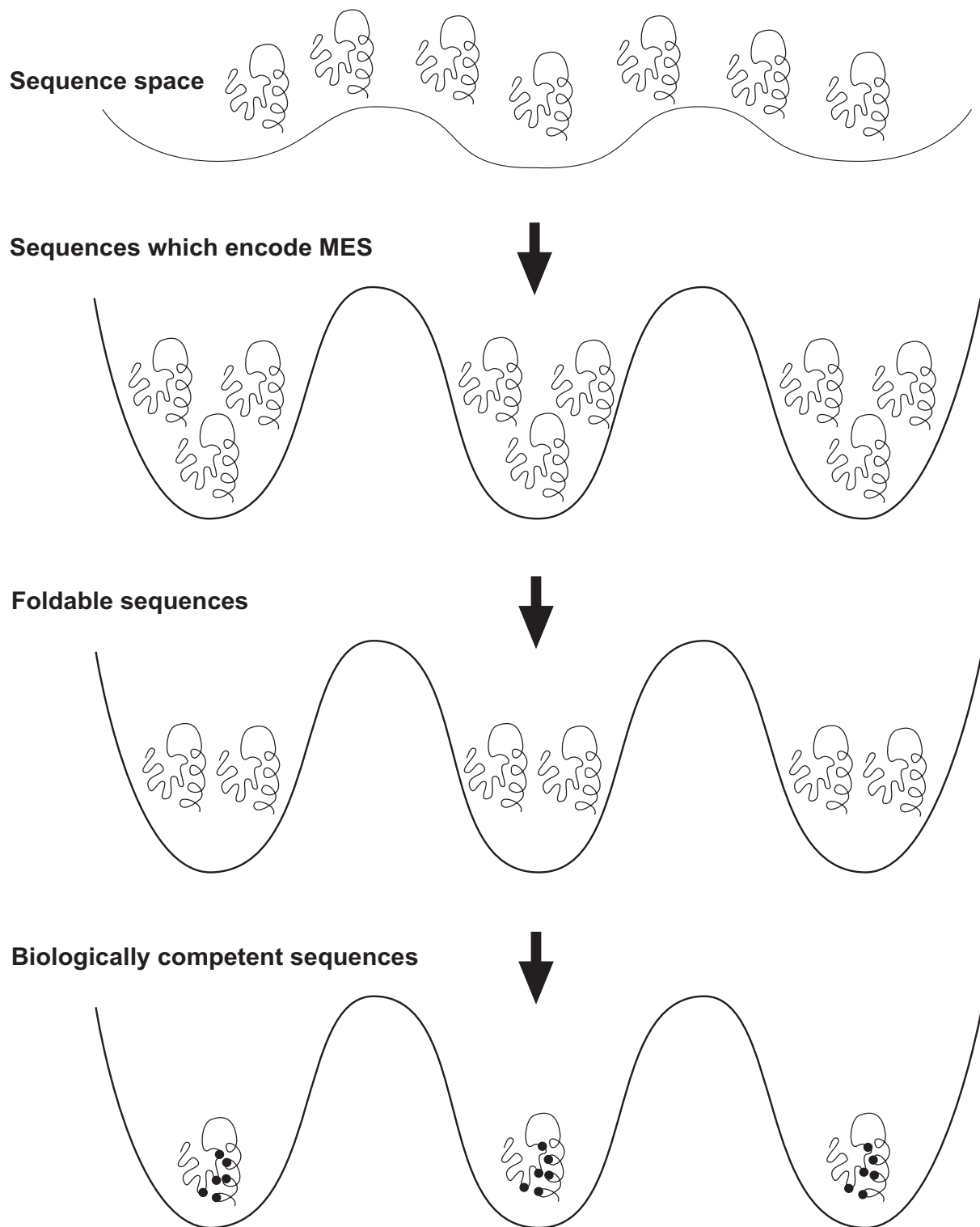


Fig. (4)

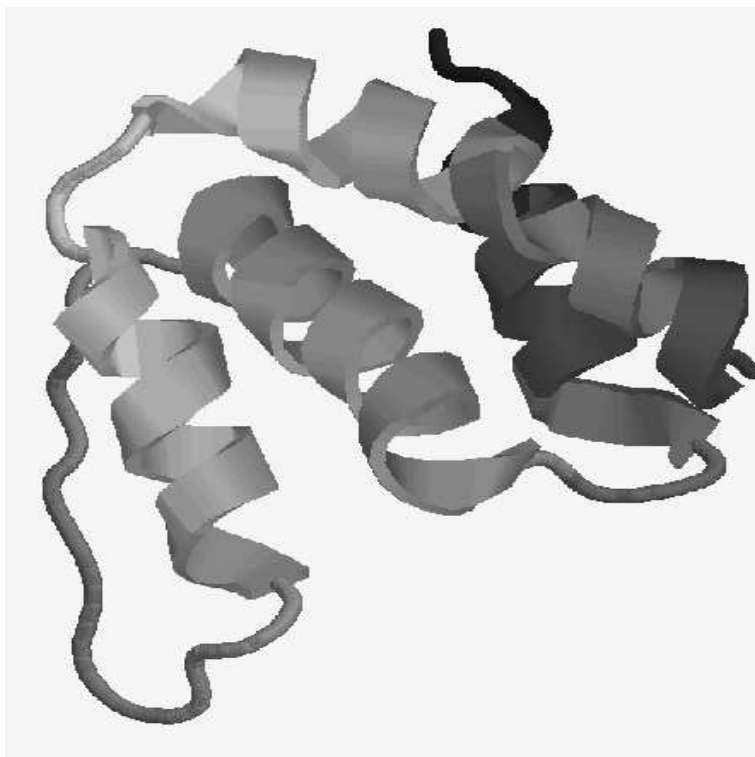


Fig. (5)

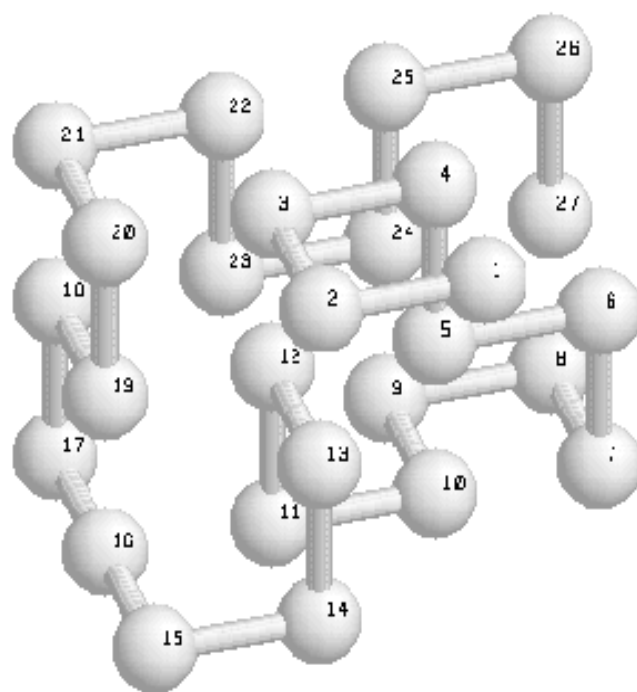


Fig. (6)

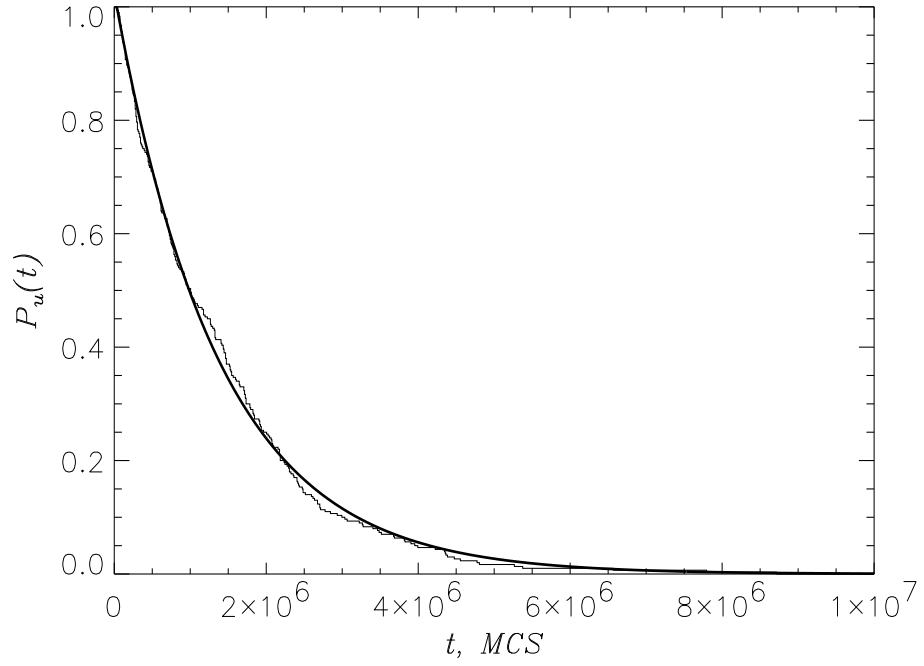
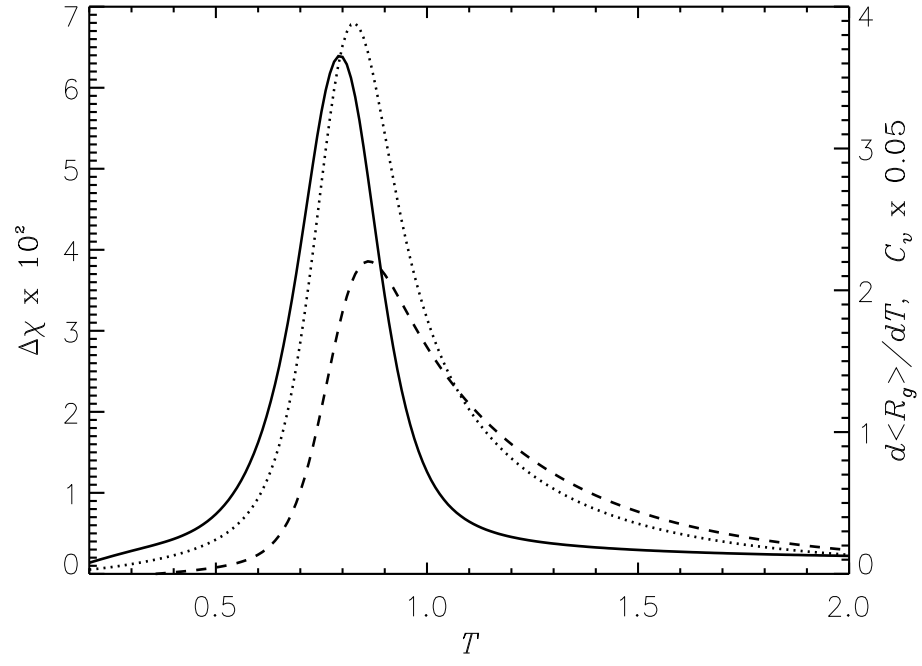


Fig. (7)

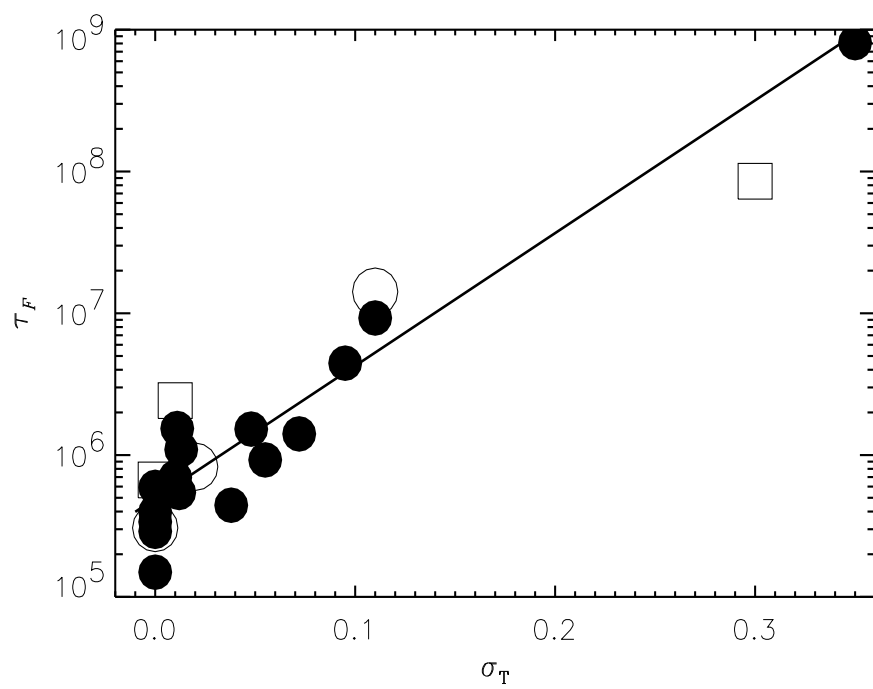


Fig. (8)

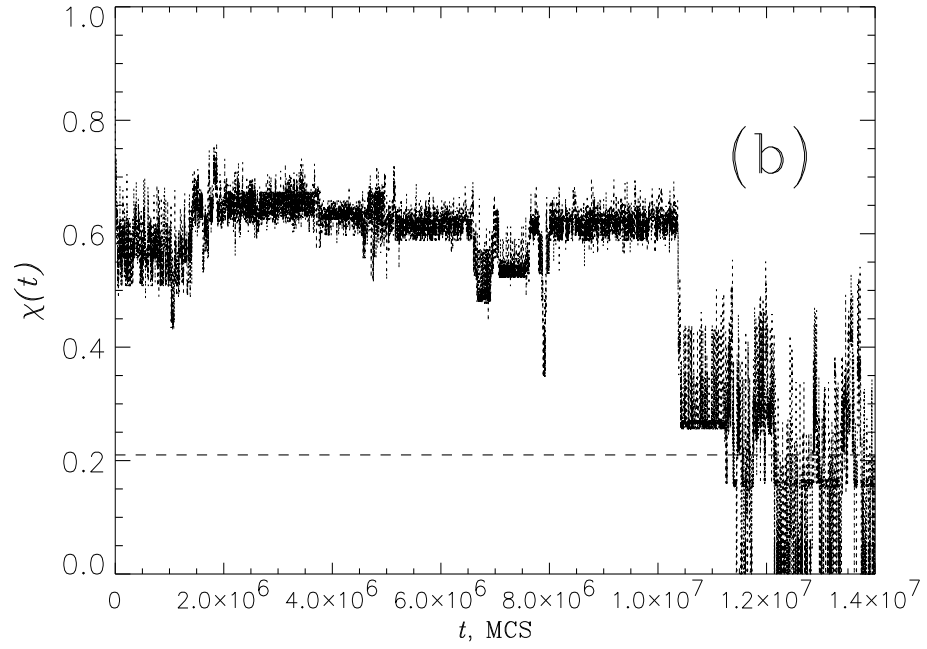
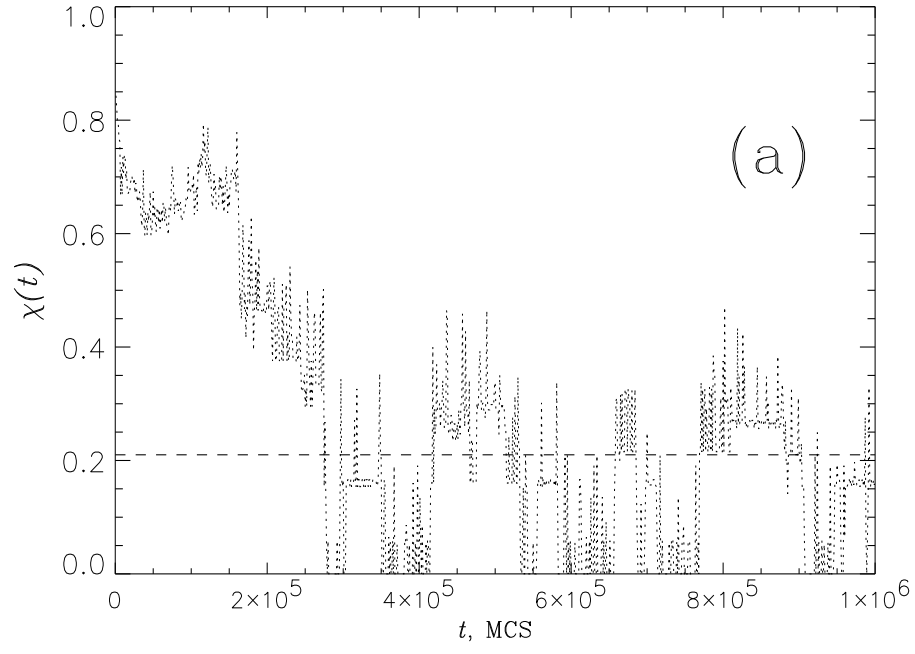


Fig. (9)

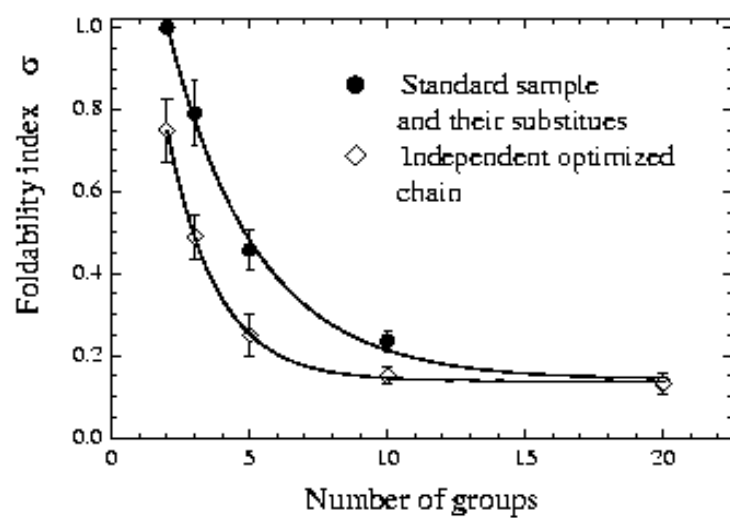


Fig. (10)